USING SATELLITE SYNTHETIC APERTURE RADAR IMAGERY TO MAP OIL SPILLS IN THE EAST CHINA SEA

Lijian Shi[1], Andrei Yu. Ivanov[1,2], Mingxia HE[1] and Chaofang Zhao[1]

[1]Ocean Remote Sensing Institute, Ocean University of China; Key Laboratory of Ocean Remote Sensing of Ministry of Education shilj@orsi.ouc.edu.cn

[2]P.P. Shirshov Institute of Oceanology, Russian Academy of Sciences, ivanoff@sio.rssi.ru

ABSTRACT ... Oil pollution of the ocean is a major environmental problem, especially in its coastal zones. Synthetic aperture radar (SAR) flown on satellites, such as ERS-2 and Envisat, has been proved to be a useful tool in oil spill monitoring due to its wide coverage, day and night, and all-weather capability. The total 120 SAR images containing oil spill over the East China Sea were collected and analyzed, ranging in date from July 23, 2002 to November 11, 2005. After preprocessed, SAR images were segmented by adaptive threshold method. The oil spill images were incorporated into GIS after distinguished from look-like phenomena, finally we presented the oil spills distribution map for the East China Sea. The wide-swath and quick-looks SAR imagery for mapping of oil spill distribution over large marine areas were proved to be useful when full resolution data are not available. After the temporal and spatial distribution of the oil spills were analyzed, we found that most of oil spills were distributed along the main ship routes, which means the illegal discharge by ships, and the occurrence of oil spill detected on SAR images acquired during morning and summer is much higher than during evening and winter.

KEY WORDS: Oil Spill, SAR, GIS, East China Sea

1. INTRODUCTION

Annually more than 100 million liters of hydrocarbon are spilled in the world's oceans. Illegal dumping associated with tank cleaning accounts for three quarters of the amount discharged (Wismann, 1993). In response to economic development, the oil requirement of China has been increasing. At the same time, the amount and tonnage of oil ship are increasing and the occurrence probability of oil spill is increasing correspondingly. Oil spill in the China Sea has become one of the most serious environmental problems.

Many researches have proved that Synthetic Aperture Radar (SAR) is the most important satellite sensor today in oil spill monitoring due to its large coverage and the ability to observe oceans at night and under cloudy weather conditions. Because of damping the short gravity-capillary waves, oil spill on the sea surface becomes visible as darkness area on radar images.

SAR images acquired by the ERS-1/2, ENVISAT and RADARSAT-1 satellites have been used extensively for obtaining statistical information on oil pollution of different sea area. For the first time, Pavlakis et al.(1996) collected a large set of SAR images over the Mediterranean Sea to study the oil spill detection. The similar researches were carried by Gade and Alpers(1999) to investigate the North Sea, Baltic Sea and the Gulf of Lion oil spills using more than 400 ERS SAR images. It was concluded that these waters were polluted mostly along main ship routes. Lu et al. (2000) compiled a statistical spatial distribution map of oil pollution for the Southeast Asian waters after analyzing about 2500 middle resolution ERS SAR images. In 2002 the demonstration of an oil spill detection/mapping capability using Radarsat Narrow ScanSAR images were implemented over the waters in the East China Sea (Ivanov et al., 2002). As a particular case, methodology for mapping oil slicks associated with the bottom seepages using GIS was presented in 2006 (Zatyagalova and Ivanov, 2006).

This paper presents and discusses the first results of the oil spill mapping project over the East China Sea. The collected SAR images were incorporated into GIS after the appearance of oil spills were emphasized, image segmented and the accurate location information obtained. Then the temporal and spatial distributions of oil spill were analyzed.

2. DATA

SAR images in the ESA web-based archive/catalogue have been used to compile the images containing oil spills in the East China Sea in 2002-2005. The total 120 SAR images (35 strips) were found in the archive, date ranging from July 23, 2002 to November 11, 2005.

Some ERS-2 and Envisat SAR images with full resolution have been ordered in ESA under the frameworks of the Dragon Project (ID:2566) and AO Envisat project #226. ERS-2 PRI images were collected with the swath of 100 km and the spatial resolution of 25m. Envisat ASAR images included the Image Mode (IM) and Wide Swath Mode (WSM). The IM product is similar to PRI of ERS-2, and the WSM product's resolution is 150m with coverage of 400×400 km^2.

The low resolution images, so-called quick-looks (QLs), were used as the secondary data to support oil spill mapping. QLs have an advantage due to the fact that the dark signatures of oil spills can still be delineated, but the small size of data files make it easier to be quickly processed. They were downloaded from the web-based

ESA EOLI ODISSEO Catalogue and from the BRSGS catalogue. The data were collected in JPEG format with pixel size of 200 m (resolution ~400 m); each QL image also covers a marine area of 100×100 km^2.

3. OIL SPILL SEGMENTATION

Detectability of oil spills in SAR images depend on both the wind and oil parameters (wind speed, spill age, oil type etc.) (Bern et al., 1992). In spite of development of automatic and semi-automatic methods of SAR image analysis, visual methods of analysis still dominates at the present time (Ivanov et al., 2002). The operational service provided today still relies on visual methods.

In our analysis, we followed the general approach: (1) SAR image preprocessing including antenna pattern/incidence angle correction and SAR image filtering, (2) image segmentation and darkness area detection, (3) discriminating the oil spill from look-like phenomena and transforming the final result into the GIS. Figure 1 shows the result for each processing step.

First step was to preprocess the SAR data, which includes denoising, resizing and removing background. The enhanced Lee filter (Lopes et al., 1990) is used to reduce speckle noise. For full resolution image, the window of size 8×8 pixels was used to compress data in order to reduce the computing time. SAR images typically have a variation in gain across the range direction due to the instrument's antenna gain difference. This gain variation can be removed by using the ENVI's Antenna Pattern Correction procedure. But due to the presence of land, the ENVI's result is not satisfying. So the background was computed by using average of 50×50 sizes window, then we get the more uniform image by original image minus background.

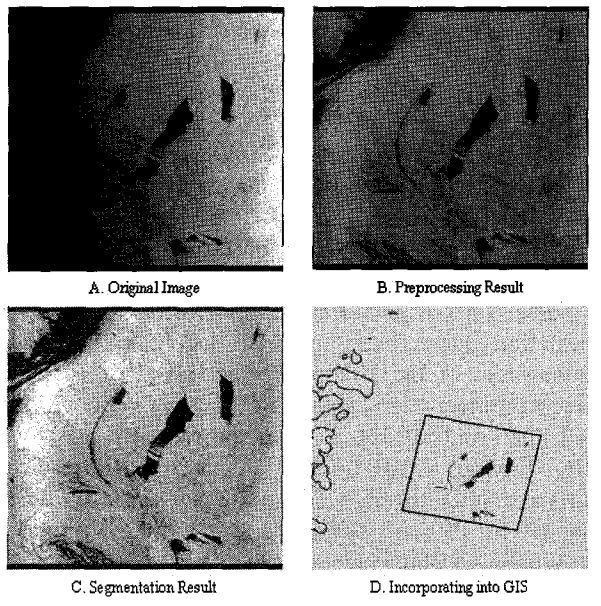

Figure 1. Processing steps (A. original image; B. preprocess; C. segment; D. distinguish oil spill and incorporate into GIS).

Second step was to segment the darkness area. Oil spills, characterized by low backscattering levels, were shown in low gray value in SAR images. Generally the histogram of SAR image with oil spill is bimodal, so the minimum value between two peak values is chosen as threshold. But sometimes the ratio of oil spill to whole image is small and the first peak of histogram is not obvious, so it's difficult to detect the minimum value between two peaks. In this case, the whole image was parted into several subsets with size 100×100 pixels and the segment method was used in each subset.

Third step was to discriminate the oil spill from look-like phenomena by manual method. In spite of development of automatic and semi-automatic methods of SAR oil spill image analysis, visual methods of analysis still dominates (Ivanov et al., 2002). The texture information (shape, area, type of edge and homogeneity) and contextual information (wind, current, location and distance to the closest bright point which is ship or platform with a certain probability) was used to distinguish oil spills from others. Finally, the result was referenced to geographic coordinates and incorporated into GIS. The control points locations, derived from definitive satellite orbital data and provided with the SAR images, were used to digitally transform the result to fit a standard map projection (Universal Transverse Mercator projection).

4. CONSTRUCTING GIS

A variety of phenomena can create the slick signatures on the SAR imagery of the sea surface, including biological surfactants (from plankton and fishes), upwelling, algal blooms, shoals and floating vegetation. Many of these phenomena can be eliminated based on its appearance of the slick (size and shape, etc.), its location relative to surrounding features (rigs, ships, etc.), its orientation relative to prevailing wind and current and other oceanic or atmospheric phenomena. Therefore, an important aid to correctly interpreting the significance of slicks is a GIS and GIS-based databases that include the locations of platforms, major shipping lanes, bathymetry, etc. The GIS provides a framework for analysis.

A GIS database for the East China Sea was compiled from data of several sources. Vector shoreline data were obtained from the NOAA's National Geophysical Data Center(NGDC)(http://rimmer.ngdc.noaa.gov/mgg/coast/getcoast.html). Bathymetric contours were extracted from the ETOPO-2 Topographic Model downloaded from the web-based archives of the University Corporation for Atmospheric Research (UCAR) (http://dss.ucar.edu/datasets/ds759.3/data).Platform locations and major shipping lanes were obtained from the East China Sea Branch of State Oceanic Administration of China (SOA) (http://www.eastsea.gov.cn/Module/Show.aspx?id=2381). All datasets were compiled using Arc GIS 9.0 software, and were placed into a geographic projection.

5. DISCUSSION

Table 1 and Figure 2 show the overpassing time distribution of SAR images. The occurrence of oil spill detected on SAR images acquired in morning (about 2:00

UTC) is much higher than in evening and is about 92% (110/120) of all images. Gade and Alpers (1999) attribute this to the fact that oil spills discharged from ships most frequently during night time can stay on the sea surface for several hours and is still visible on SAR images acquired during morning passes. In addition, the sea surface temperature is high on the daytime and the viscosity of water become low, so the contrast of SAR image is larger and it's easier to detect the oil spill. Moreover, about 77% (92/120) of the all images are acquired during the summer months (from April to September) especially July (30) and August (31), because compared with winter time, the wind speed in China Sea is lower and the sea surface temperature is higher during summer and oil spill is easier to be detected.

	Quicklooks	Full resolution
Total number of SAR images		
ERS	63	12
ASAR	17	28
	Morning(about 2:00 UTC)	Evening(about 11:00 UTC)
	110	10

Table 1. Details of the collected SAR images.

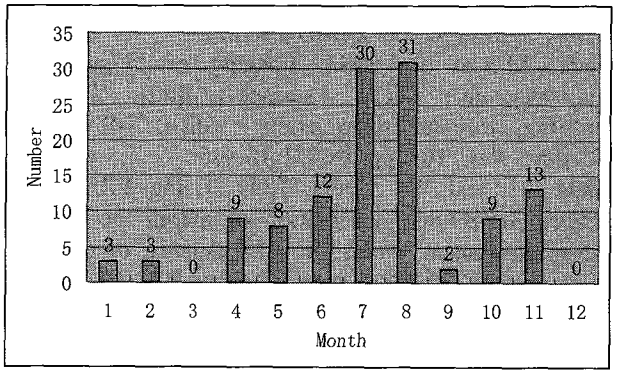

Figure 2. Bar chart of the number of SAR images during different month.

Figure 3A shows an ERS-2 SAR image acquired over the East China Sea on August 12 2004, at 2:26 UTC. On the right part of the image there are many oil spills with linear shape which caused by illegal discharge, where two ships could be found obviously. The length of oil spill is about 90km. The longest oil trail shows a "feathered" structure, which was caused by wind. The heavy component of oil is located downwind and appears darker line in the image. The wind direction arrow in the image was deduced from the instruction of the longest oil trail, which is consistent with the result from QuikScat.

Among oil spills, slicks formed by fish oil or mixture of fish oil and oil products can be found sometimes (Clemente-Colón, 2002). Figure 3B, acquired by ERS-2 on 28 August 2004, 2:24UTC, shows the oil slicks associated with fishing operations in the mouth of Yangtze River which is the one of primary fishing ground of the East China Sea. The slicks present the distinctive patterns because of reverse or return moving of fishing ships during operations. Many ships can be found around the slicks.

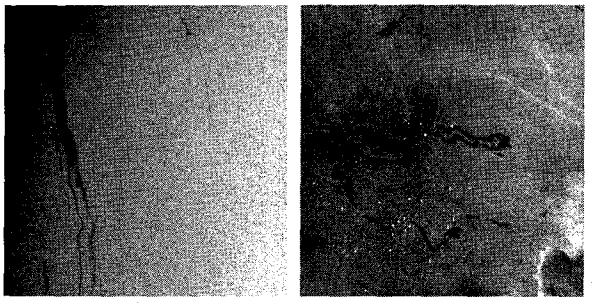

A B

Figure 3. ERS-2 SAR images of the China Sea. The left shows the oil spill caused by ship's oil discharge; the right shows fishing spills with high probability.

SAR image is also very useful to distinguish seepage slicks from sea bottom (Zatyagalova and Ivanov, 2006). Seepages, especially in prolifically seeping regions, can be found repetitiously at the same location on SAR images acquired at different times and passes. In Figure 4 shows two ASAR images which was acquired on 25 August 2004, 1:50UTC and 28 August 2004, 1:56UTC. The images show the slicks with nested shape caused by natural seepage with high probability. There is a good overlapping between SAR images acquired on 25 and 28.08 2004, and the imaged slicks most probably have the same source on the bottom.

Figure 5 presents the oil distribution map over the China Sea, which consists with the major regional shipping lanes very well. This result is similar to the findings reported in Gade and Alpers(1999), Lu et al.(2000) and Ivanov et al.(2002) for the European, South Asian and Chinese waters repectively. The most polluted zones are detected in central part of the Yellow Sea around 31-37°N latitudes and 122-124°E longitudes and lies in the intersection of several major shipping lanes such as from Shanghai to Dalian/Yantai. The second polluted zone is near the Bohai Strait in the north part of the Yellow Sea. The zone below the Yangtze River is also heavily polluted. In this area there are many linear type oil spill caused by ships' illegal discharge along the shipping routes.

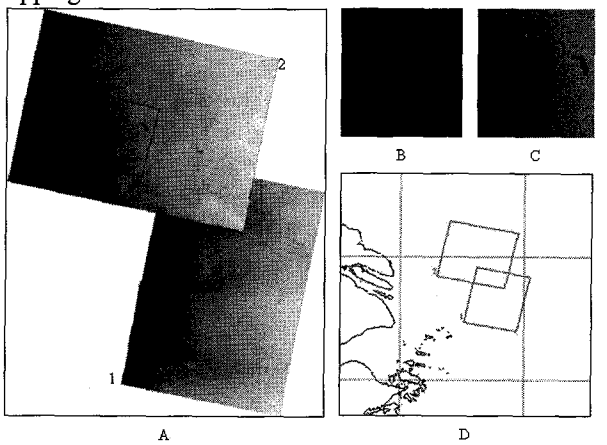

Figure 4. The slicks with nested shape caused by natural seepage with high probability. A. two ASAR images of

the China Sea; B, C: the detail of oil spills; D, the location of oil spills.

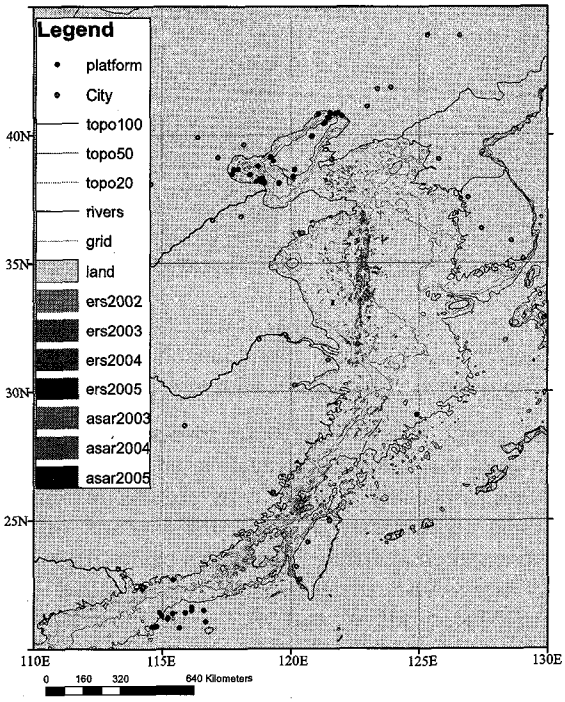

Figure 5. Oil spill distribution map for the East China Sea.

The number of collected SAR images is still not enough for spatial distribution. For example , there are no oil spills over the Liaodong Bay and Laizhou Bay of Bohai Sea in the map, but actually the pollution of these area is serious. Otherwise, few oil spills are found in the sea area around Qingdao of the distribution map where there are many ship lanes to Qingdao.

6. CONCLUSIONS

Based on collection and analysis of the different swath and resolution SAR imagery and making a GIS as framework, the oil spills distribution map for the Yellow Sea and East China Sea was presented. Below most important findings of the study are summarized.

1. The wide-swath and quick-looks SAR imagery for mapping of oil spill distribution over large marine areas are proved useful when full resolution data are not available.

2. In East China Sea, most oil spills are caused by ships' illegal discharge. There are some other type oil spills such as natural seepage, fishing production waste.

3. The most serious polluted zone is the central part of the Yellow Sea with limited by 31-37°N latitudes and 122-124°E longitudes. The most oil spills are distributed along the shipping routes, which is similar to the findings reported in Gade and Alpers(1999), Lu et al.(2000) and Ivanov et al.(2002).

4. The occurrence of oil spill detected on SAR images acquired during morning and summer is much higher than it during evening and winter.

5. The number of collected SAR images is still not enough and distribution over some area is not exact. So much more SAR images are needed to be collected and processed in order to obtain more accurate information about oil spill distribution and risk areas in the China Seas.

Aknowledgements

This research was carried out in the frameworks of the Dragon Project (ID2566) and AO Envisat project #226 at the Ocean Remote Sensing Institute (Ocean University of China) with financial support from the Key Laboratory of Ocean Remote Sensing of Ministry of Education and Ocean University of China. We are very grateful to ESA for the timely acquisition, processing and delivery of the SAR images.

References

Brekke, C. and A.H.S. Solberg, 2005. Oil spill detection by satellite remote sensing. *Remote Sensing of Environment*, 95, pp. 1-13.

Clemente-Colón, P., 2002. The use of Spaceborne Synthetic Aperture Radar in the Monitoring and Management of Bering Sea Fisheries. *Scientific and Operational Applications of Remote Sensing for Coastal and Marine Fisheries*, Morales J. and D. Blackburn. UNESCO CSI Info Paper 14.

Espedal, H.A., et al., 1998. COSTWATCH'95 ERS 1/2 SAR detection of natural film on the ocean surface. *J. Geophys. Res.*, 92, pp. 24,969-24,982.

Gade, M., et al., 1998. Imaging of biogenic and anthropogenic ocean surface films by the multifrequency/multipolarization SIR-C/X-SAR. *J. Geophys. Res.*, 103, pp. 18,851-18,866.

Gade, M. and W. Alpers, 1999. Using ERS-2 SAR images for routine observation of marine pollution in European coastal waters. In: *The Science of the Total Environment* 237/238. Elsevier Science B.V. London, pp. 441-448.

Ivanov, A., M.-X. He and M.-Q. Fang, 2002. Oil spill detection with the RADARSAT SAR in the waters of the Yellow and East China Sea: A case study. *Proc. ACRS-2002 - 23rd Asian Conference on Remote Sensing*, 25-29, Kathmandu, Nepal.

Lopes, A., R. Touzi and E. Nezry 1990. Adaptive speckle filters and Scene heterogeneity. *IEEE Trans. Geosci. Rem. Sens.*, 28, 6, pp. 992-1000.

Lu, J., et al., 2000. Mapping oil pollution from space. *Backscatter*, 11(1), pp. 23-26.

Pavlakis, P., Sieber, A. And Alexandry, S., 1996. Monitoring oil spill pollution in the Mediterranean with ERS SAR. *Earth Observation Quarterly*, 52, pp. 13-16.

Solberg, A.H.S. and R. Solberg 1997. A large-scale evaluation of features for automatic detection of oil spills in ERS SAR images. *Proc. IGARSS'97*, v. 3, pp. 1484-1486.

Wismann V. 1993. Radar signatures of mineral oil spills measured by an airborne multi-frequency radar and the ERS-1 SAR. *Proc. IGARSS'93*, pp. 940-942.

Zatyagalova, V. and A. Ivanov 2006. Using Envisat ASAR images to detect and characterize hydrocarbon seeps in the Caspian Sea. *Proc. EUSAR-2006 Conference*, 16-18 May 2006, Dresden, Germany.